© 2023. Published by The Company of Biologists Ltd | Development (2023) 150, dev200857. doi:10.1242/dev.200857

RESEARCH ARTICLE

CNKSR2, a downstream mediator of retinoic acid signaling, modulates the Ras/Raf/MEK pathway to regulate patterning and invagination of the chick forebrain roof plate

Niveda Udaykumar[1], Mohd Ali Abbas Zaidi[1,*], Aishwarya Rai[1] and Jonaki Sen[1,2,‡]

ABSTRACT

During embryonic development, the forebrain roof plate undergoes invagination, leading to separation of the cerebral hemispheres. Any defects in this process, in humans, lead to middle interhemispheric holoprosencephaly (MIH-HPE). In this study, we have identified a previously unreported downstream mediator of retinoic acid (RA) signaling, *CNKSR2*, which is expressed in the forebrain roof plate in the chick embryo. Knockdown of *CNKSR2* affects invagination, cell proliferation and patterning of the roof plate, similar to the phenotypes observed upon inhibition of RA signaling. We further demonstrate that *CNKSR2* functions by modulating the Ras/Raf/MEK signaling. This appears to be crucial for patterning of the forebrain roof plate and its subsequent invagination, leading to the formation of the cerebral hemispheres. Thus, a set of novel molecular players have been identified that regulate the morphogenesis of the avian forebrain.

KEY WORDS: *CNKSR2*, Retinoic acid signaling, Chick embryo, Ras/Raf/MEK signaling, Patterning, Forebrain

INTRODUCTION

During the development of the forebrain, the invagination of the roof plate results in the generation of the two cerebral hemispheres from a single telencephalic vesicle. Defects in the invagination of the roof plate often lead to congenital disorders such as middle interhemispheric holoprosencephaly (MIH-HPE) in humans, which causes seizures and intellectual disabilities (Roessler and Muenke, 2010; Weiss et al., 2018). Several genes encoding signaling molecules or transcription factors have been implicated in the etiology of HPE (Dubourg et al., 2007; Dupe et al., 2011; Geng and Oliver, 2009; Ishiguro et al., 2018; Keaton et al., 2010; Krauss, 2007; Nanni et al., 1999; Petryk et al., 2015; Ribeiro et al., 2006). Despite this, there is a lack of comprehensive knowledge about the molecular mechanisms and downstream targets through which these genes regulate the process of separation of the cerebral hemispheres.

We observed that, in the chick forebrain, the roof plate invaginates as a W-shaped structure (Fig. 1J). Previously, we identified RA signaling as one of the regulators of the invagination of the chick forebrain roof plate and showed that the kink or loop of the W expresses *Bmp7*, while the lateral arms express *Wnt7b*, *Zic2* and *Otx2*. We have also reported that the inhibition of RA signaling leads to a flattened forebrain roof plate, which is similar to the phenotype observed in HPE (Gupta and Sen, 2015). One major question emerging from this was: how does RA signaling regulate forebrain roof plate invagination in the chick embryo? The answer to this question would shed light on the etiology of MIH-HPE.

In this study, we identify *CNKSR2* (connector enhancer kinase suppressor of Ras 2) as being expressed in a similar domain to RA signaling in the forebrain roof plate midline. Therefore, we investigated *CNKSR2* as a novel downstream mediator of RA signaling during forebrain roof plate invagination. The expression of *CNKSR2* in the developing chick forebrain was first reported in a genome-wide screen examining the expression patterns of metabolism-related genes during embryonic development (Roy et al., 2013). Before this, CNKSR2 was identified as a scaffold protein and a modulator of Ras/Raf/MEK signaling, through a mutagenesis screen in *Drosophila melanogaster* (Therrien et al., 1998). In humans, mutations in *CNKSR2* are associated with seizures, attention, language deficits and X-linked neurodevelopmental disorders (Damiano et al., 2017; Daoqi et al., 2020; Houge et al., 2011; Sun et al., 2018; Vaags et al., 2014), and neurodevelopmental delay (Higa et al., 2021). Recently, loss of *CNKSR2* in male mice has been shown to cause behavioral changes, with increased neural activity and alterations in the synaptic proteome (Erata et al., 2021). This underscores the importance of understanding the role of *CNKSR2* and the underlying process(s) that are affected by its knockdown during vertebrate nervous system development.

To characterize the function of *CNKSR2* in the chick forebrain roof plate, we employed a RNAi-based method to knockdown the transcript. We observed that loss-of-function of *CNKSR2* leads to invagination defects, with the appearance of increased cell proliferation and an increase in phosphorylated MEK1/2 (pMEK1/2)-positive cells in the roof plate midline. Furthermore, knockdown of *CNKSR2* was observed to affect the patterning of the invaginating forebrain roof plate through the alteration of the expression of roof plate markers such as *Bmp7*, *Wnt7b*, *Zic2* and *Otx2*. Thus, our results show that *CNKSR2*, when acting downstream of RA signaling, is a regulator of both patterning and invagination of the forebrain roof plate through its modulation of Ras/Raf/MEK signaling.

RESULTS

Spatiotemporal expression profiling of *CNKSR2* and active RA signaling in the forebrain roof plate

A genome-wide expression screen for metabolism-related genes (MRGs), based on whole-mount RNA *in situ* hybridization of chick

[1]Department of Biological Sciences and Bioengineering, Indian Institute of Technology Kanpur, Kanpur 208016 Uttar Pradesh, India. [2]Mehta Family Center for Engineering in Medicine (MFCEM), Indian Institute of Technology Kanpur, Kanpur 208016, Uttar Pradesh, India.
*Present address: Department of Neurological Sciences, University of Nebraska Medical Center, Omaha, NE 68198, USA.

‡Author for correspondence (jonaki@iitk.ac.in)

N.U., 0000-0002-0709-1473; J.S., 0000-0001-7316-6376

Handling Editor: François Guillemot
Received 13 April 2022; Accepted 3 January 2023

Development (2023) 150, dev200857. doi:10.1242/dev.200857

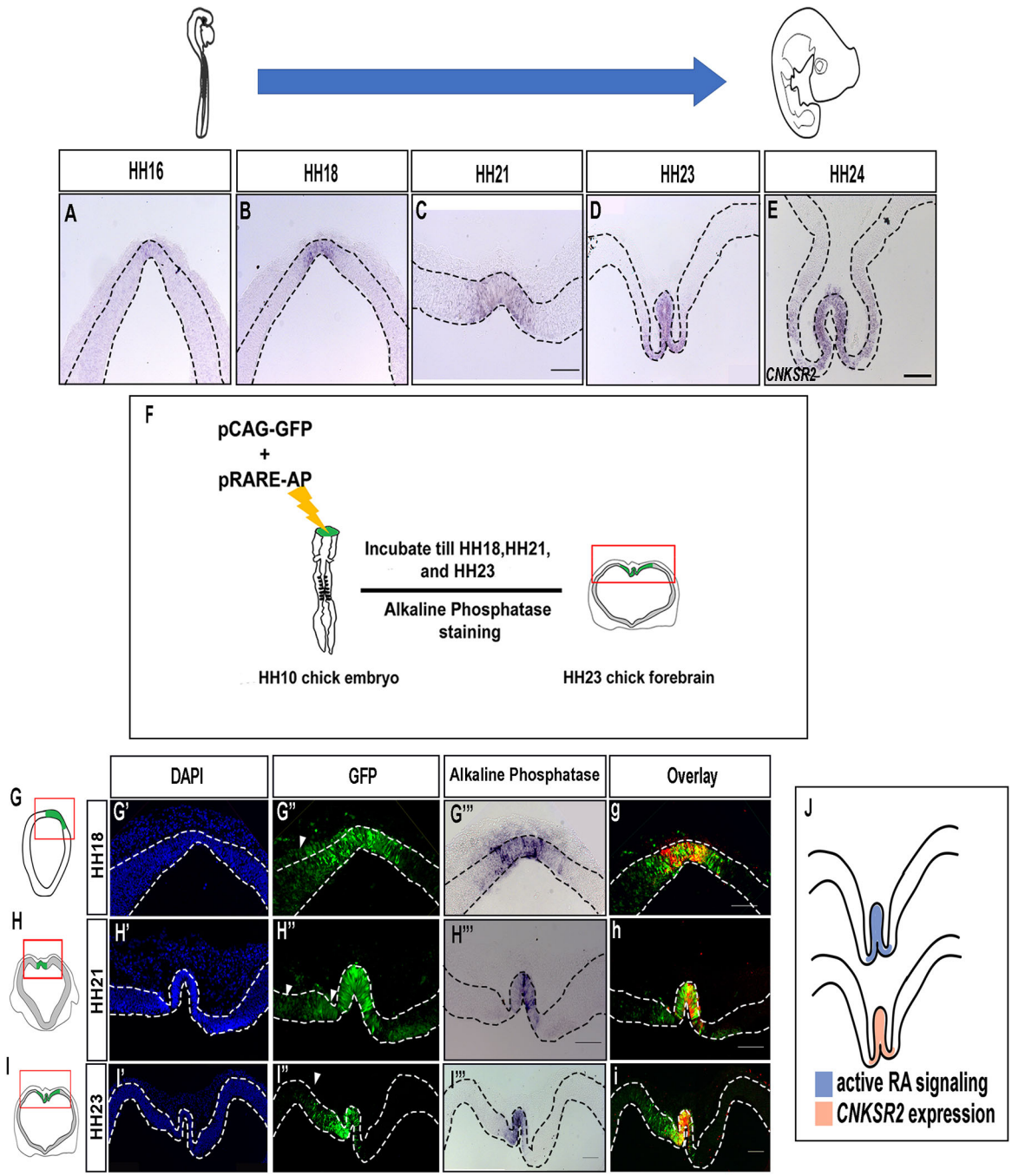

Fig. 1. The domains of active retinoic acid signaling and expression of *CNKSR2* coincide in the invaginating forebrain roof plate. (A-E) Expression of *CNKSR2* in the invaginating forebrain roof plate at (A) HH16, (B) HH18, (C) HH21, (D) HH23 and (E) HH24. (F) Experimental strategy for detecting active RA signaling in the forebrain roof plate at HH23. The same strategy is applied for stages HH18 and HH21. (G,H,I) Schematic illustrations of chick forebrain sections at HH18 (G), HH21 (H) and HH23 (I). The red boxes indicate the regions indicated in the photomicrographs on the right. (G′,H′,I′) DAPI staining (blue) of the forebrain roof plate at HH18 (G′), HH21 (H′) and HH23 (I′). (G″,H″,I″) GFP (green) shows the extent of electroporation with GFP in the HH18 (G″), HH21 (H″) and HH23 (I″) forebrains (white arrowheads indicate GFP-positive cells not showing AP staining). (G‴,H‴,I‴) Alkaline phosphatase (AP) staining indicates the domain of active RA signaling. (g,h,i) Pseudo color images of GFP (green) and AP staining (red). (J) Schematic illustration depicting the regions of active RA signaling and the expression of *CNKSR2* at the HH23 forebrain roof plate. Scale bars: 50 µm in C; 100 µm in A,B,D,E,G-I. *n*=3 for all experiments in this figure.

embryos, identified *CNKSR2* as one of the genes expressed in the forebrain (Roy et al., 2013). Our attention was specifically drawn to *CNKSR2*, as its expression domain appeared to coincide with the domain of active RA signaling in the forebrain roof plate midline, which has previously been reported to regulate forebrain roof plate invagination (Gupta and Sen, 2015). Thus, to investigate further, we performed a spatiotemporal expression analysis of *CNKSR2* by RNA *in situ* hybridization. The *CNKSR2* transcripts could be first detected at low levels in the midline of the chick forebrain at stages HH16 (Hamburger and Hamilton, 1951) and HH18 (Fig. 1A,B). At stages HH21-HH24, it was robustly expressed in the midline (loop of W) of the invaginating roof plate (Fig. 1C-E). From the

Development (2023) 150, dev200857. doi:10.1242/dev.200857

spatiotemporal expression profiling, it appeared that the expression of *CNKSR2* overlapped the domain of active RA signaling (Gupta and Sen, 2015). To confirm this, we electroporated a reporter construct for RA signaling (pRARE-AP) in the dorsal roof plate at HH10 and analyzed its expression at HH18, HH21 and HH23 (Fig. 1F). Alkaline phosphatase activity, indicating active RA signaling, was detected to be in a domain overlapping the expression of *CNKSR2* in the roof plate at these stages (Fig. 1G-Jg-i). Based on this, we hypothesized that the expression of *CNKSR2* is likely to be regulated by RA signaling in the context of the invaginating forebrain roof plate of the chick embryo.

The expression of *CNKSR2* is regulated by RA signaling in the forebrain roof plate

We performed gain- and loss-of-function studies of RA signaling to determine whether the expression of *CNKSR2* is indeed regulated by RA signaling. The constitutively active RA receptor pCIG-VP16RARα-IRES-GFP (Gupta and Sen, 2015) was electroporated in the lateral chick forebrain at HH18 to activate RA signaling ectopically (Fig. 2A). At HH23, GFP^+ cells indicate the region of electroporation and the cells that expressed the constitutively active RA receptor. RNA *in situ* hybridization for *CNKSR2* revealed that it is now expressed ectopically in the lateral forebrain, in addition to its normal domain of expression in the roof plate midline (Fig. 2C-C″), when compared to control electroporated lateral forebrain (Fig. 2B-B″). This demonstrated that activation of ectopic RA signaling in the chick forebrain is sufficient for inducing the expression of *CNKSR2* in the lateral chick forebrain.

To create loss of function of RA signaling in the forebrain roof plate, the dominant-negative RA receptor, pCAGEN-RAR403 (Gupta and Sen, 2015), was electroporated in the forebrain roof plate at HH10 (Fig. 2D). We observed that the loss of RA signaling in the invaginating roof plate leads to the absence of *CNKSR2* transcript, as detected by RNA *in situ* hybridization (Fig. 2G-G″,g, *n*=5), in comparison to control, pCAG-GFP (Fig. 2F-F″,f, *n*=5), suggesting that *CNKSR2* is regulated by RA signaling.

Knockdown of *CNKSR2* affects the invagination of the forebrain roof plate

To investigate whether *CNKSR2* acts as the downstream mediator of RA signaling to regulate the invagination of the forebrain roof plate, we knocked down the transcript of *CNKSR2* using a RNAi-based approach. Two RNAi constructs were designed to target *CNKSR2* RNA and were cloned into the pRmiR vector (Smith et al., 2009). The efficiency of the knockdown was tested through an *in vitro* sensor assay (Sindhu et al., 2019) (Fig. S1). One of these constructs, *CNKSR2*-RNAi (1), was the most efficient in knocking down the *CNKSR2* transcript. This construct was used for subsequent analyses and is referred to as *CNKSR2*-RNAi. The knockdown construct was electroporated into the forebrain roof plate at HH10 and harvested at HH23, the stage where invagination defects can be best scored. We found a dramatic decrease in expression of *CNKSR2* in the *CNKSR2*-RNAi electroporated forebrains (Fig. 3C-E‴) compared with the control (control pRmiR-empty) electroporated forebrains (Fig. 3B-B‴), indicating efficient knockdown (Fig. 3A).

Knockdown of *CNKSR2* in the forebrain roof plate led to varying degrees of defects in invagination. In control embryos, the forebrain roof plate was observed to invaginate as a W-shaped structure with the expression of *CNKSR2* restricted to the middle loop of the W (Fig. 3B-B‴). However, upon knockdown of *CNKSR2*, depending on the extent of electroporation, the morphology of the invaginating forebrain roof plate was altered. In the embryos with a relatively higher extent of electroporation, we observed a nearly flattened roof plate (Fig. 3C-C‴, *n*=13/29) which closely resembled the phenotype observed upon inhibition of RA signaling (Gupta and Sen, 2015). Furthermore, in the embryos with a moderate extent of electroporation, we observed the invagination to be U/V-shaped instead of a W-shaped structure (Fig. 3D-E‴, *n*=16/29). Quantification of the percentages of occurrences of the phenotypes upon knockdown of *CNKSR2* showed a higher occurrence of the U/V roof plate than the flattened roof plate (Fig. 3F). However, we observed no change in RA signaling in the forebrains with the knockdown of *CNKSR2* (Fig. S2, *n*=3). In addition, analysis of apoptotic cells by TUNEL assay at HH18 (Fig. S3A-B″,E) and HH23 upon knockdown of *CNKSR2* in the roof plate did not show any significant statistical difference (Fig. S3C-D″,F). This observation rules out the role of cell death as a contributor to the invagination defects seen upon knockdown of *CNKSR2*.

Knockdown of *CNKSR2* increases cell proliferation in the invaginating forebrain roof plate

The inhibition of RA signaling led to an increase in cell proliferation in the forebrain roof plate midline (Gupta and Sen, 2015). To determine whether *CNKSR2* might be functioning downstream of RA signaling to regulate cell proliferation in the forebrain roof plate, we knocked down the *CNKSR2* mRNA, followed by immunostaining for phospho-histone 3 (PH3) (Fig. 4A). We observed that, in the control, pRmiR-empty electroporated forebrains, the PH3-positive cells were higher in the lateral arms of the W and low in the middle loop (Fig. 4B-B″), whereas in the *CNKSR2*-RNAi electroporated forebrains, the distribution of the PH3-positive cells was uniformly high throughout the roof plate (Fig. 4C-C″). In addition, quantification of the percentage of PH3-positive cells in the roof plate midline of the test and control electroporated forebrains showed a statistically significant difference (*n*=5 each for test and control) (Fig. 4D).

To further confirm whether *CNKSR2* regulates cell proliferation in the forebrain roof plate, we used EdU labeling to detect proliferating cells after knockdown of *CNKSR2*, according to the strategy described in Fig. 4E. We observed that, although in the control there were very few EdU-positive cells in the middle of the W when compared with the lateral sides (Fig. 4F-G″), in the test (*CNKSR2*-RNAi) a relatively higher number of EdU-positive cells was observed throughout the roof plate (Fig. 4H-I″). Quantification of the percentage of EdU-positive cells in the test and control electroporated forebrains showed a statistically significant difference between the two (Fig. 4J, *n*=5 each for test and control). These experiments suggested that cell proliferation in the forebrain roof plate is regulated by the *CNKSR2*.

Because we observed a change in cell proliferation upon knockdown of *CNKSR2*, we wanted to determine whether ectopic expression of *CNKSR2* would be sufficient for regulating cell proliferation. For this, we expressed mouse *CNKSR2* (m*CNKSR2*) by electroporating pCAG-m*CNKSR2* in the lateral region of the chick forebrain at HH18, followed by analysis at HH23 (Fig. S4A). The expression of m*CNKSR2* in the electroporated samples was assessed by RNA *in situ* hybridization with a probe specific for m*CNKSR2* (Fig. S4B-C″, *n*=3). However, ectopic expression of m*CNKSR2* in the lateral chick forebrain did not result in a decrease in cell proliferation in this region (Fig. S4D-F, *n*=4, each for test and control).

Knockdown of *CNKSR2* alters the patterning of the forebrain roof plate

We found that the misexpression of m*CNKSR2* did not alter cell proliferation in the lateral forebrain; however, changes in cell

Development (2023) 150, dev200857. doi:10.1242/dev.200857

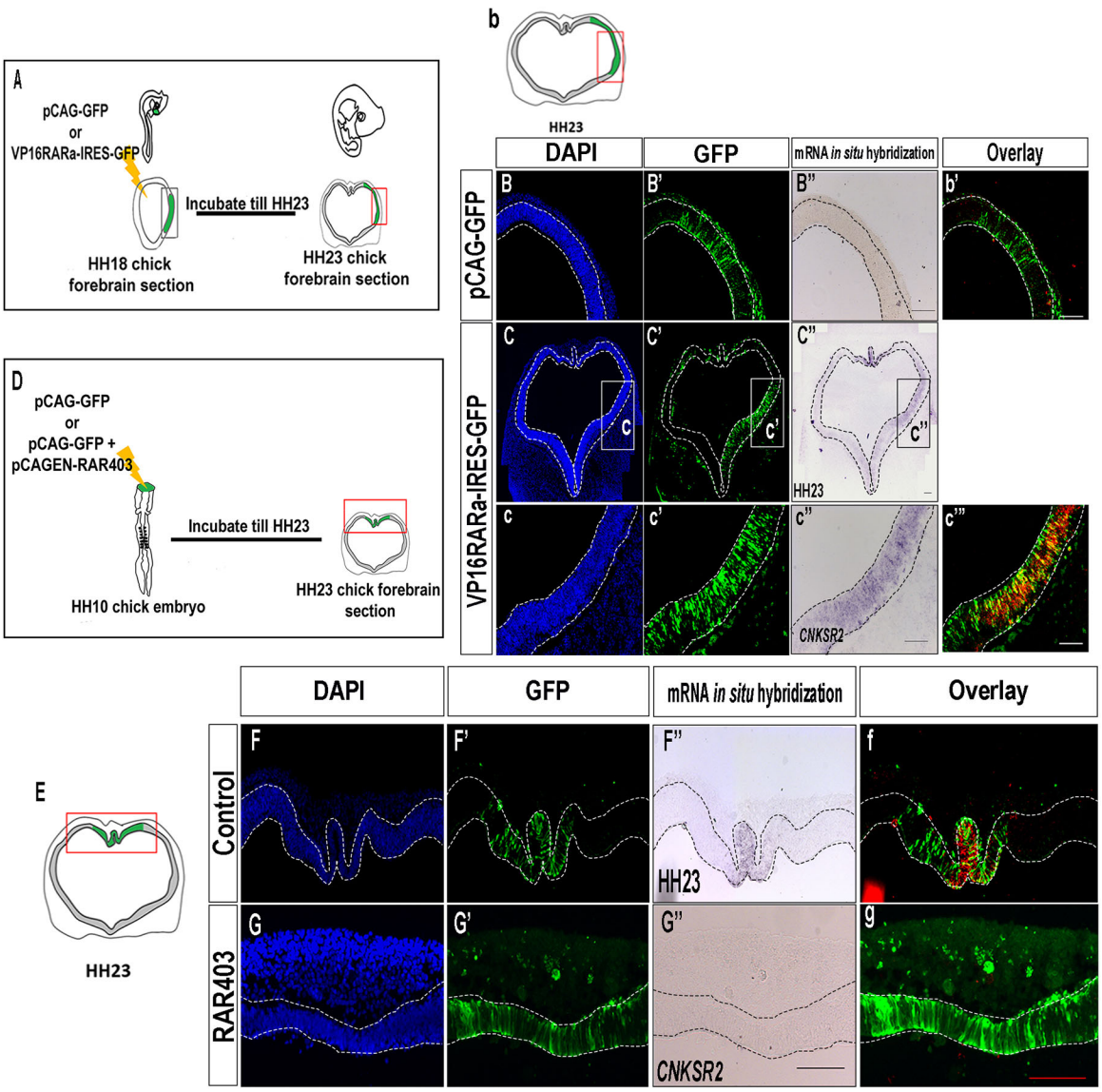

Fig. 2. RA signaling regulates the expression of *CNKSR2* in the invaginating forebrain roof plate. (A) Experimental strategy for the ectopic activation of RA signaling by electroporating VP16RARα-IRES-GFP in the lateral chick forebrain. (b) Schematic illustration of the HH23 chick forebrain. The red box indicates the region shown in the photomicrographs below. (B,C) DAPI staining (blue) of the control (B) and VP16RARα-IRES-GFP-electroporated (C) forebrain section. (B′,C′) GFP (green) shows the extent of electroporation of pCAG-GFP (B′) and VP16RARα-IRES-GFP (C′) in the lateral chick forebrain. (B″,C″) mRNA *in situ* hybridization showing the expression of *CNKSR2* transcript (B″) and *CNKSR2* (C″). (b′) Pseudo color images of GFP (green) and *CNKSR2* transcript (red) of control electroporated embryos. (c-c″) Magnified images of the boxed regions in C-C″. (c‴) Pseudo color images of GFP (green) and *CNKSR2* transcript (red) of test electroporated embryos. (D) Experimental strategy for inhibiting RA signaling using dominant-negative RA receptor (pCAGEN-RAR403). (E) Schematic illustration of the HH23 chick forebrain. The red box indicates the region shown in the photomicrographs on the right. (F,G) DAPI staining (blue) of pCAG-GFP (F) and pCAGEN-RAR403 (G) electroporated chick forebrain roof plate at HH23. (F′,G′) GFP (green) shows the extent of electroporation of pCAG-GFP (F′) and pCAGEN-RAR403 (G′) in the forebrain roof plate. (F″,G″) mRNA *in situ* hybridization of *CNKSR2* on the pCAG-GFP (F″) and pCAGEN-RAR403 (G″) electroporated samples showing the absence of *CNKSR2* expression after pCAGEN-RAR403 electroporation (G″). (f) Pseudo-color images of GFP (green) and *CNKSR2* transcript (red) of control electroporated embryos. (g) Pseudo-color images of GFP (green) and *CNKSR2* transcript (red) of test electroporated embryos. Scale bars: 100 µm. *n*=5 for all experiments in this figure.

proliferation were observed in the midline upon knockdown of *CNKSR2*. Thus, we reasoned that changes in cell proliferation observed in the midline could be an indirect outcome of patterning changes in the forebrain roof plate. We have previously observed that inhibition of RA signaling in the forebrain roof plate leads to patterning defects with changes in expression of the roof plate markers *Bmp7*, *Wnt7b*, *Zic2* and *Otx2*. For example, there was a loss of expression of *Bmp7* and a shortening of the expression domains of *Wnt7b*, *Zic2* and *Otx2* upon inhibition of RA signaling (Gupta and Sen, 2015). Thus, we investigated whether the knockdown of *CNKSR2* affects the expression of these markers similarly.

In the control forebrains, some of these markers exhibit unique expression patterns within the roof plate (Fig. 5A). For example, *Bmp7* expression was found to be restricted to the middle loop of the W (Fig. 5B-B″), while *Wnt7b* (Fig. 5D-D″) was expressed at higher levels in the lateral arms of the W (black arrowheads in Fig. 5D″) when compared with the middle loop (red arrowheads in Fig. 5D″). On the other hand, *Zic2* and *Otx2* exhibited relatively uniform

Development (2023) 150, dev200857. doi:10.1242/dev.200857

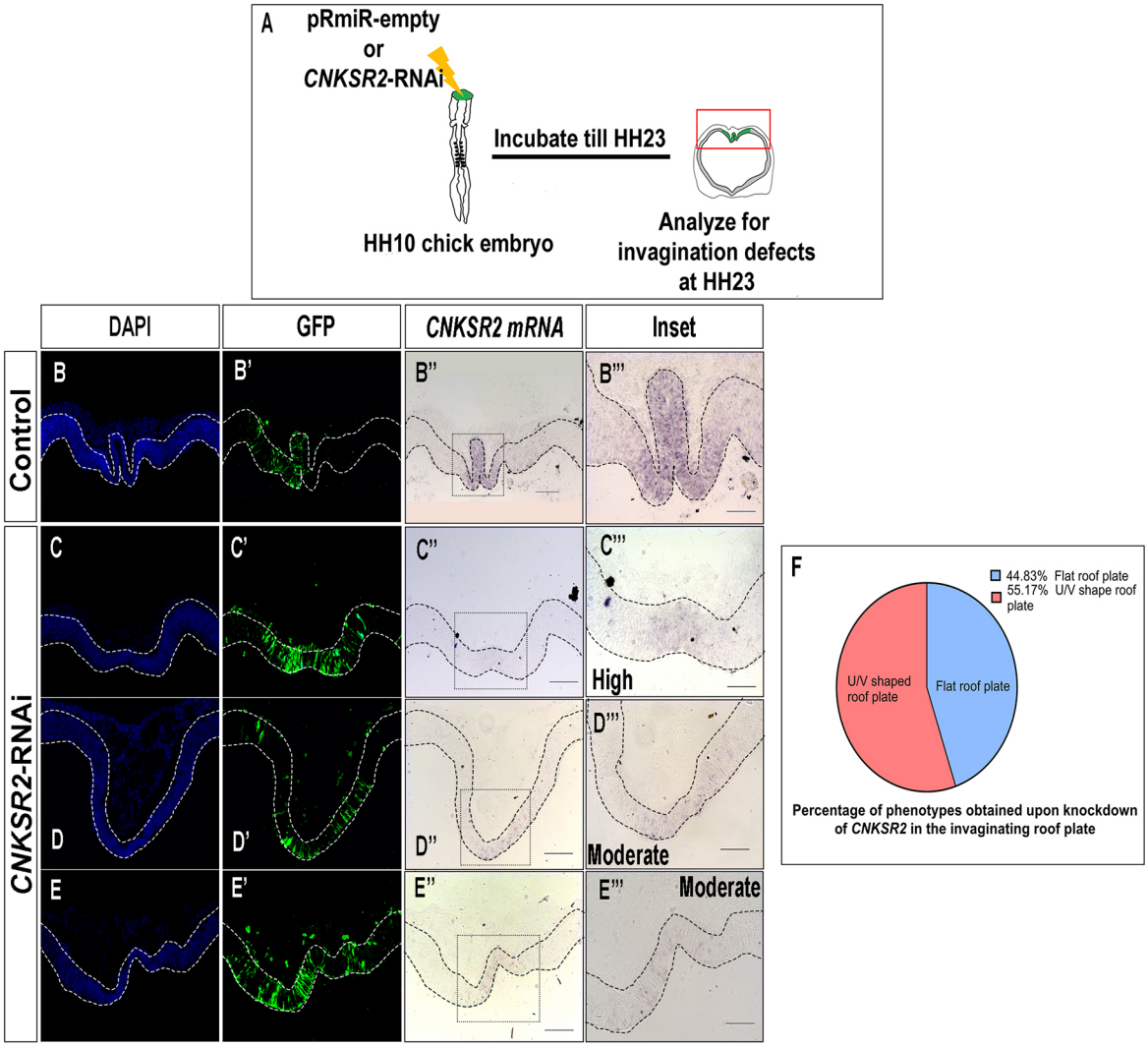

Fig. 3. Knockdown of *CNKSR2* in the invaginating roof plate leads to invagination defects. (A) Experimental strategy for the knockdown of *CNKSR2* in the invaginating chick forebrain. The red box indicates the region shown in the photomicrographs below. (B,C,D,E) DAPI staining (blue) of the control pRmiR-empty electroporated chick forebrain section (B), the test *CNKSR2*-RNAi electroporated chick forebrain section with an almost flattened roof plate (C), the test *CNKSR2*-RNAi electroporated chick forebrain section with U/V roof plate (D) and the test *CNKSR2*-RNAi electroporated chick forebrain section with U/V roof plate (E). (B′,C′,D′,E′) GFP showing the extent of electroporation of the pRmiR-empty vector (B′), the broad extent of electroporation of the *CNKSR2*-RNAi (C′), the moderate extent of electroporation of the *CNKSR2*-RNAi (D′) and the moderate extent of electroporation of the *CNKSR2*-RNAi (E′). (B″,C″D″,E″) mRNA *in situ* hybridization of *CNKSR2* on the pRmiR-empty electroporated samples (B″), *CNKSR2* on the *CNKSR2*-RNAi electroporated samples (C″), *CNKSR2* on the *CNKSR2*-RNAi electroporated samples (D″) and *CNKSR2* on the *CNKSR2*-RNAi electroporated samples (E″). (B‴,C‴,D‴,E‴) The regions outlined in B″,C″,D″,E″ at higher magnification. (F) Pie chart showing the percentage of occurrence of the two phenotypes upon knockdown of *CNKSR2* in the roof plate. Scale bars:100 µm in B-B″,C-C″,D- D″ and E-E″; 50 µm in B‴,C‴,D‴ and E‴. *n*=5 each for control and test in A-E‴; *n*=29 in F.

expression across the W-shaped roof plate (Fig. 5F-F″,H-H″). Upon knockdown of *CNKSR2*, we observed that there was a dramatic decrease in the expression of *Bmp7* (Fig. 5C-C″). Similarly, the midline expression domain of *Wnt7b* was absent, with only expression in the lateral arms of the W remaining (Fig. 5E-E″). On examining the expression of *Zic2* (Fig. 5G-G″, the extent of expression marked by the black arrowheads) and *Otx2* (Fig. 5I-I″, the extent of expression marked by the black arrowheads), we found a shortening of the domains of expression of these two markers (Fig. 5J). These changes in expression of *Bmp7*, *Wnt7b*, *Zic2* and *Otx2* were remarkably similar, if not identical, to those observed upon inhibition of RA signaling (Gupta and Sen, 2015). Thus, the changes in expression of roof plate markers may be interpreted as altered patterning, as the morphology of the roof plate itself was altered from a W-shaped invagination to either a flattened or U/V-shaped invagination, with the middle loop of the W missing. Furthermore, we observed that ectopic expression of m*CNKSR2* in the lateral forebrain (Fig. 5K) was sufficient for inducing the expression of *Bmp7* (Fig. 5L-M″, *n*=5 each for control and test), *Zic2* (Fig. S5A-C″), *Wnt7b* (Fig. S5D-E″) and *Otx2* (Fig. S5F-G″, *n*=3 each for control and test) in this ectopic location.

CNKSR2 regulates the invagination of the forebrain roof plate by modulating Ras/Raf/MEK signaling

CNKSR2 has been reported to modulate the Ras/Raf/MEK signaling (Sundaram and Han, 1995; Therrien et al., 1998); hence, we decided to investigate whether *CNKSR2* functions similarly in the forebrain roof plate. To detect the status of Ras/Raf/MEK signaling, we performed immunostaining for pMEK1/2. We observed that, in the forebrains electroporated with control

Development (2023) 150, dev200857. doi:10.1242/dev.200857

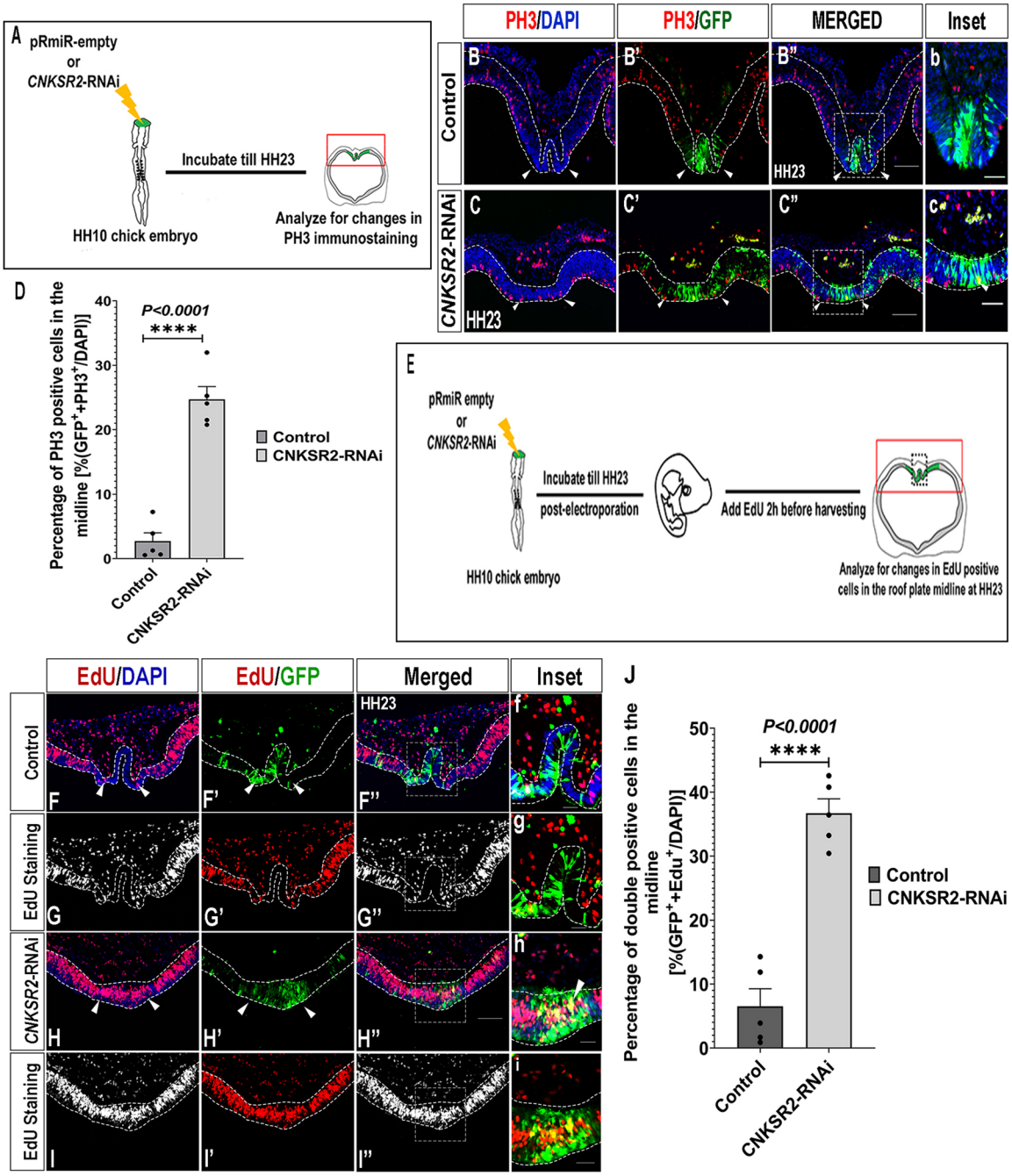

Fig. 4. Knockdown of *CNKSR2* affects cell proliferation in the invaginating roof plate midline. (A) Experimental strategy for analyzing cell proliferation by PH3 immunostaining in the invaginating roof plate midline upon knockdown of *CNKSR2*. (B,C) DAPI (blue) and PH3 immunostaining (red) on pRmiR-empty electroporated forebrain (B) and *CNKSR2*-RNAi electroporated forebrain (C). Arrowheads indicate low PH3-positive cells in the invaginating roof plate midline in comparison with the flanks (B) and uniform PH3-positive cells in the invaginating roof plate midline (C). (B′,C′) GFP (green) and PH3 immunostaining (red) showing the extent of electroporation of pRmiR-empty (B′) and *CNKSR2*-RNAi (C′) in the roof plate. Arrowheads indicate low PH3-positive cells in the electroporated region (B′) and uniform PH3-positive cells in the electroporated region (C′). (B″,C″) Merged images of B and B′, C and C′. Arrowheads indicate low PH3-positive cells in the electroporated region (B″) and uniform PH3-positive cells in the electroporated region (C″). (b,c) The regions outlined in B″,C″ at higher magnification. (D) Quantification of the percentage of PH3-positive cells in the invaginating roof plate midline between control and *CNKSR2*-RNAi electroporated samples. Data are mean±s.e.m. (E) Experimental strategy for analyzing cell proliferation by EdU labeling in the invaginating roof plate midline upon knockdown of *CNKSR2*. (F,H) DAPI (blue) and EdU-labeled cells (red) on the chick roof plate section of control pRmiR-empty electroporated forebrain (F) and *CNKSR2*-RNAi electroporated forebrain (H). Arrowheads indicate few EdU-positive cells in the invaginating roof plate midline compared with the flanks (F) and uniform EdU-labeled cells in the invaginating roof plate midline compared with the flanks (H). (F′,H′) GFP (green) showing the extent of electroporation of pRmiR-empty (F′) and *CNKSR2*-RNAi (H′) in the roof plate. (F″,H″) Merged images of F and F′, H and H′. (f,h) The regions outlined in F″,H″ shown at higher magnification. Arrowheads indicate double-positive (yellow) EdU labeled cells in the invaginating roof plate midline compared with the flanks. (G,I) Grayscale images of EdU staining in control (G) and test (I) samples. (G′,I′) EdU labeled cells (red) in the control (G′) and in *CNKSR2*-RNAi (I′) electroporated forebrains. (G″,I″) Grayscale images of EdU staining in control (G″) and in *CNKSR2*-RNAi (I″) electroporated forebrains. (g,i) The regions outlined in G″,I″ shown at higher magnification. (J) Quantification of the percentage of EdU-positive cells in the invaginating roof plate midline between control and *CNKSR2*-RNAi electroporated samples. ****P<0.0001 (unpaired two-tailed *t*-test using GraphPad software). Data are mean ±s.e.m. Scale bars: 100 µm. n=5 each for control and test.

Development (2023) 150, dev200857. doi:10.1242/dev.200857

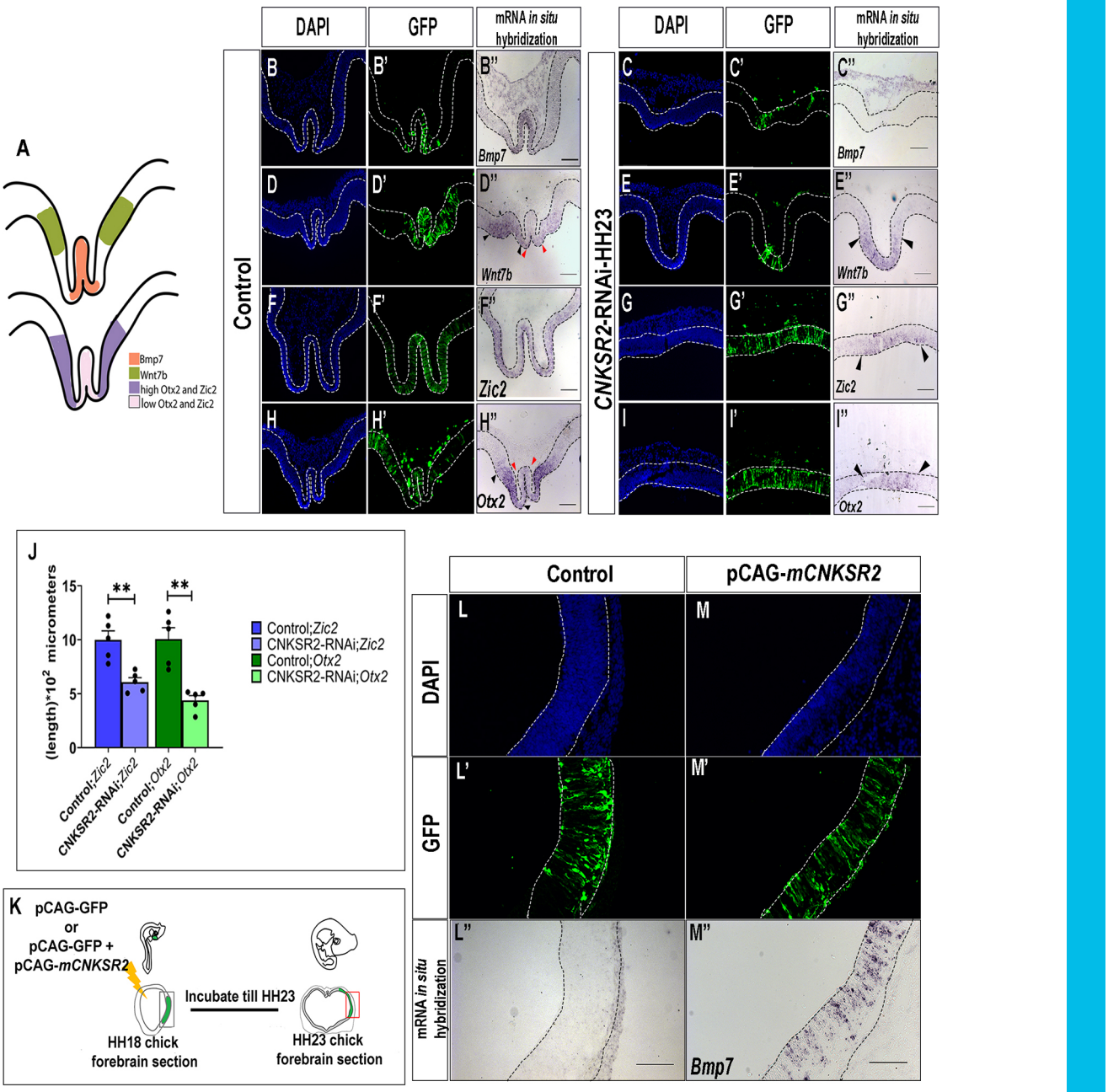

Fig. 5. Knockdown of *CNKSR2* leads to patterning defects in the invaginating roof plate. (A) Schematic illustration showing the expression domains of the roof plate markers *Bmp7*, *Wnt7b*, *Zic2* and *Otx2* in the HH23 chick forebrain. (B-I) DAPI staining (blue) of pRmiR-empty (B,D,F,H) and *CNKSR2*-RNAi (C,E,G,I) electroporated chick forebrain roof plate. (B′-I′) GFP (green) showing the extent of electroporation of pRmiR-empty (B′,D′,F′,H′) and *CNKSR2*-RNAi (C′,E′,G′,I′). (B″-I″) *Bmp7* (B″,C″), *Wnt7b* (D″,E″), *Zic2* (F″,G″) and *Otx2* (H″,I″) expression in the pRmiR-empty (B″,D″,F″,H″) and *CNKSR2*-RNAi (C″,E″,G″,I″) electroporated forebrain roof plate. In D″,H″, black arrowheads indicate high expression whereas red arrowheads indicate low expression. In E″, black arrowheads indicate uniform expression. In G″,I″, arrowheads indicate the expression domain. (J) Quantification of the expression domains of *Zic2* and *Otx2* on control and test electroporated samples. Statistical analysis was performed using an unpaired *t*-test with Welch's correction (two-tailed) between test and control. Data are mean±s.e.m.; *Zic2*, ***P*=0.0056; *Otx2*, ***P*=0.0038. (K) Experimental strategy for the misexpression of m*CNKSR2* in the lateral chick forebrain. (L,M) DAPI staining (blue) of the control pCAG-GFP (L) and pCAG-m*CNKSR2* (M) electroporated lateral forebrain. (L′,M′) GFP showing the extent of electroporation of pCAG-GFP (L′) and pCAG-m*CNKSR2* (M′). (L″,M″) *Bmp7* expression in pCAG-GFP (L″) and pCAG-m*CNKSR2* (M″) electroporated lateral chick forebrain. Scale bars:100 µm. *n*=5 each for control and test.

pRmiR-empty, pMEK1/2-positive cells were low in the midline of the forebrain roof plate but present uniformly in the ventricular zone that flanks the invaginating roof plate (Fig. 6A-A″). However, in the embryos electroporated with *CNKSR2*-RNAi, we found a statistically significant increase in pMEK 1/2-positive cells in the roof plate midline (Fig. 6B-B″,C, *n*=5 each for test and control).

As the knockdown of *CNKSR2* increased the number of pMEK1/2-positive cells in the roof plate, we wanted to determine whether modulation of the Ras/Raf/MEK signaling could rescue the defects observed in the forebrain roof plate. To do this, we co-electroporated pCIG-MKK1dn (pCIG-MKK1dn-IRES-GFP; Delfini et al., 2005) together with the *CNKSR2*-RNAi

Development (2023) 150, dev200857. doi:10.1242/dev.200857

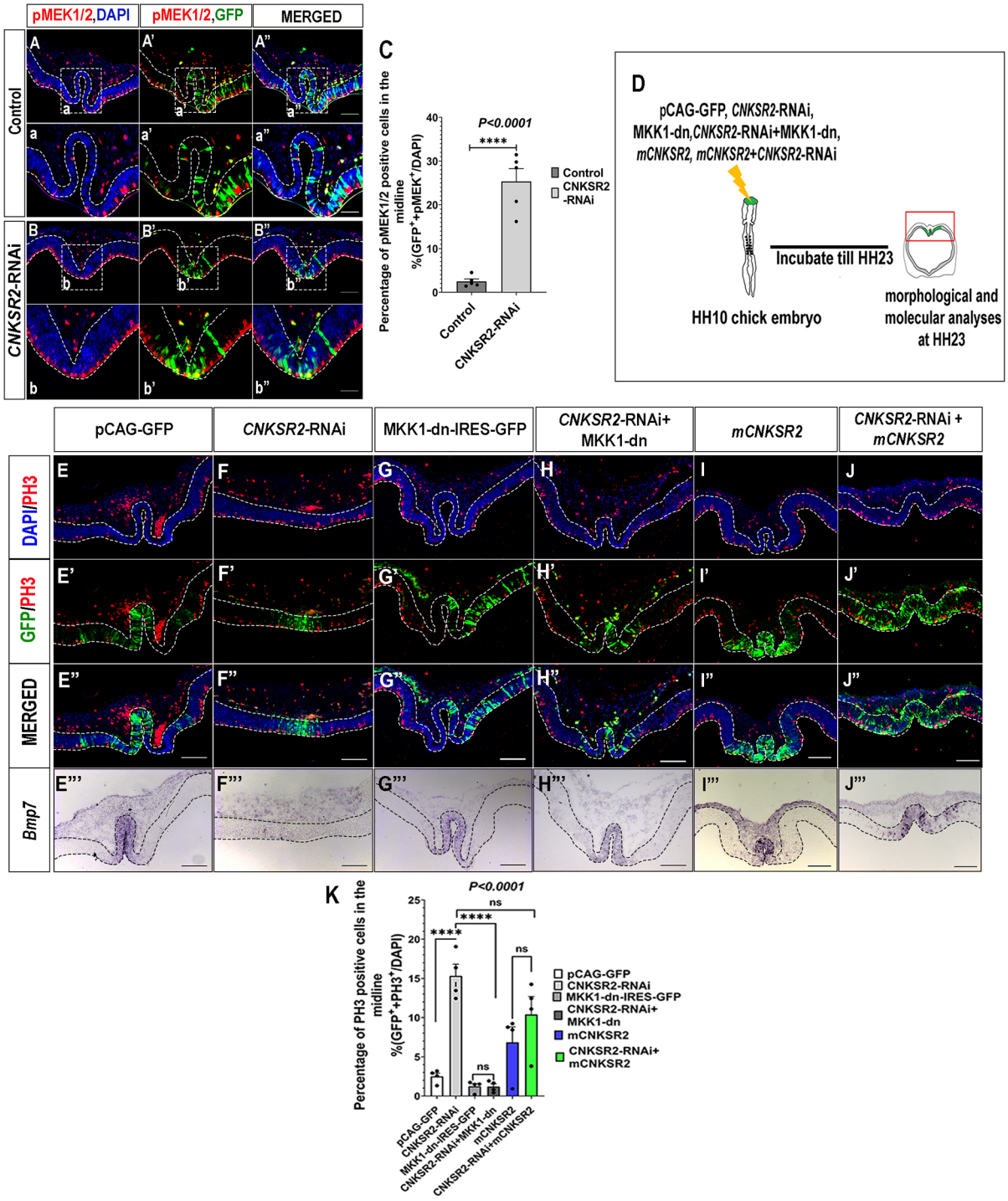

Fig. 6. *CNKSR2* modulates Ras/Raf/MEK signaling in the invaginating forebrain roof plate. (A) DAPI staining (blue) and pMEK1/2 immunostaining (red) of pRmiR-empty (A) and *CNKSR2*-RNAi (B) electroporated forebrains. (A′,B′) GFP (green) and pMEK1/2 immunostaining (red) of pRmiR-empty and *CNKSR2*-RNAi electroporated forebrains. (A″,B″) Merged images of A and A′, B and B′. (a-a″,b-b″) The regions outlined in A-A″,B-B″ at higher magnification. (C) Quantification of the percentage of pMEK1/2-positive cells in the roof plate midline between pRmiR-empty and *CNKSR2*-RNAi electroporated samples. ****P<0.0001. Data are mean±s.e.m. (D) Schematic illustration of the experimental strategy for examining the rescue of molecular and morphological changes upon knockdown of *CNKSR2*. (E-J) DAPI (blue) and PH3 immunostaining (red) of pCAG-GFP (E), *CNKSR2*-RNAi (F), MKK1dn-IRES-GFP (G), *CNKSR2*-RNAi+MKK1dn (H), m*CNKSR2*+GFP (I) and *CNKSR2*-RNAi+m*CNKSR2* (J) electroporated forebrains. (E′-J′) GFP (green) and PH3 immunostaining (red) of pCAG-GFP (E′), *CNKSR2*-RNAi (F′), MKK1dn (G′), *CNKSR2*-RNAi+MKK1dn (H′), m*CNKSR2*+GFP (I′) and *CNKSR2*-RNAi+m*CNKSR2* (J′) electroporated forebrains. (E″-J″) Merged images of E,E′-J,J′. (E‴-J‴) *Bmp7* expression in pCAG-GFP (E‴), *CNKSR2*-RNAi (F‴), MKK1dn (G‴), *CNKSR2*-RNAi+MKK1dn (H‴), m*CNKSR2*+GFP (I‴) and *CNKSR2*-RNAi+m*CNKSR2* (J‴) electroporated forebrains. (K) Quantification of the percentages of PH3-positive cells across the six conditions. Statistical analysis was carried out using one-way ANOVA across the six conditions. Data are mean±s.e.m., ****P<0.0001. Multiple comparison by Sidak's test: pCAG-GFP versus *CNKSR2*-RNAi (****P<0.0001), MKK1-dn-IRES-GFP versus *CNKSR2*-RNAi+MKK1-dn [P>0.9999 (ns)], m*CNKSR2* versus *CNKSR2*-RNAi+m*CNKSR2* [P=0.3740 (ns)], *CNKSR2*-RNAi versus *CNKSR2*-RNAi+MKK1-dn (****P<0.0001), *CNKSR2*-RNAi versus *CNKSR2*-RNAi+m*CNKSR2* [P=0.1107 (ns)]. Scale bars: 50 µm in a-a″ and b-b″; 100 µm A-A″,B-B″ and E-J‴. n=5 each for control and test in A-b″. n=4 each for control and test in E-J″. n=3 each for E‴-J‴.

Development (2023) 150, dev200857. doi:10.1242/dev.200857

in the HH10 chick forebrain and compared it with the forebrains electroporated with the controls pCAG-GFP, *CNKSR2*-RNAi and pCIG-MKK1dn, and assessed the rescue of the invagination defect by observing the morphology. For rescue of the patterning defects, we examined the expression of the midline marker *Bmp7*; for changes in cell proliferation, we performed PH3 immunostaining (Fig. 6D-H‴, n=4 for control and test). We found that in the forebrains electroporated with pCIG-MKK1dn and *CNKSR2*-RNAi+MKK1dn, the invagination of the roof plate, the reduced cell proliferation in the midline (Fig. 6G-G″,H-H″) and the expression of the midline marker *Bmp7* (Fig. 6G‴,H‴) were comparable with that of the control (electroporated with pCAG-GFP) (Fig. 6E-E‴), indicating a rescue. Conversely, the forebrains electroporated with *CNKSR2*-RNAi showed invagination defects, increased cell proliferation and reduced *Bmp7* expression (Fig. 6F-F‴). We assessed for knockdown of *CNKSR2* by RNA *in situ* hybridization in the samples co-electroporated with *CNKSR2*-RNAi and MKK1-dn, and found there was knockdown and rescue due to expression of MKK1-dn (Fig. S6).

To determine whether the phenotype observed after knockdown of *CNKSR2* was not due to off-target effects, we attempted to rescue the knockdown by expressing *mCNKSR2* in the forebrain roof plate. Forebrains co-electroporated with *CNKSR2*-RNAi and *mCNKSR2* showed partial rescue in terms of invagination, cell proliferation (n=4) and *Bmp7* expression (n=3) (Fig. 6J-J‴) when compared with forebrains electroporated with *mCNKSR*2 alone (Fig. 6I-I‴, n=4 for PH3 and n=3 for *Bmp7*).

With respect to cell proliferation, a partial rescue was observed with co-electroporation of *CNKSR2*-RNAi and *mCNKSR2* as this lowered the percentage of PH3-positive cells in the midline when compared with that of the forebrain midline electroporated with *CNKSR2*-RNAi alone. In fact, the lower percentage of PH3-positive cells in the roof plate midline was similar to that observed in forebrains electroporated with pCAG-GFP, MKK1-dn, *CNKSR2*-RNAi+MKK1dn and *mCNKSR2* (Fig. 6K).

However, we observed that misexpression of MKK1-dn in the lateral chick forebrain did not alter the number of PH3-positive cells compared with control (Fig. S7A-B″), but interestingly was sufficient to induce the expression of roof plate midline marker *Bmp7* (Fig. S7D-D″) in this ectopic location compared with control (Fig. S7C-C″). Thus, these experiments indicate that *CNKSR2* modulates Ras/Raf/MEK signaling in the forebrain roof plate, which appears to be necessary for its invagination.

Because loss of RA signaling leads to invagination defects (Gupta and Sen, 2015), and in this study we have established that *CNKSR2* is a downstream target of RA signaling in this context (Fig. 2), we wanted to investigate whether *mCNKSR2* can rescue the forebrain midline invagination defects observed upon inhibition of RA signaling. We observed that simultaneous loss of RA signaling by co-electroporation of pCAGEN-RAR403 (dominant-negative RA receptor) and pCAG-*mCNKSR2* did not rescue the invagination defect seen upon loss of RA signaling (Fig. S8D-E′, n=3 for each). The presence of *mCNKSR2* was assayed by RNA *in situ* hybridization (Fig. S8A-C′). These experiments suggest that *CNKSR2* may not be the sole downstream mediator of RA signaling in this context, and there may be other as yet unidentified targets that regulate the process of midline invagination in the chick forebrain.

Furthermore, we observed that constitutive activation of Ras/Raf/MEK signaling in the forebrain roof plate through the expression of HRasV12 (electroporation of pcDNA3-HRasV12) leads to invagination defects (Fig. S9B-B″) when compared with the control (pCAG-GFP) electroporated forebrain (Fig. S9A-A″), suggesting a crucial role of this pathway in forebrain roof plate morphogenesis.

DISCUSSION

In this study, we have compared a comprehensive spatiotemporal expression profiling of *CNKSR2* with that of active RA signaling at stages HH18, HH21 and HH23, and found that the two domains overlap to a large extent. In addition, an *in silico* analysis of a 2 kb upstream region of chicken *CNKSR2* showed the presence of the consensus half-sites [PuG(G/T)TCA] for RA signaling (see Fig. S10). This supports our hypothesis that RA signaling regulates the expression of *CNKSR2* in this context. Furthermore, we observed an alteration in the expression of *CNKSR2* upon manipulation of RA signaling through loss- and gain-of-function experiments. Taken together, this led us to conclude that *CNKSR2* is a downstream mediator of RA signaling in the chick forebrain roof plate.

We observed that the knockdown of *CNKSR2* in the forebrain roof plate leads to invagination defects. Whenever the electroporation of the RNAi construct spanned a broad domain, an almost flattened roof plate was observed. This prompted us to determine the underlying causes of the invagination defects upon knockdown of *CNKSR2*. We reasoned that one likely cause for this could be an abolition of the differences in cell proliferation that normally exists in the roof plate. The rationale behind this is as follows: (1) we have previously shown that RA signaling regulates cell proliferation in the forebrain roof plate (Gupta and Sen, 2015); (2) evidence from the literature suggests that RA signaling can regulate the mitogen-activated protein kinase (MAPK) pathway (Crowe et al., 2003; Nakagawa et al., 2003; Wang and Yen, 2008), which in turn is known to regulate cell proliferation; and (3) CNKSR2 is a scaffolding protein and has been shown to modulate the Ras/Raf/MEK pathway (Sundaram and Han, 1995; Therrien et al., 1998). We thus hypothesized that RA signaling regulates cell proliferation through *CNKSR2* and its modulation of Ras/Raf/MEK signaling.

When we assessed cell proliferation and the status of Ras/Raf/MEK signaling upon the knockdown of *CNKSR2* in the forebrain roof plate, we found an increase in cell proliferation and pMEK1/2-positive cells in the midline. Interestingly, misexpression of mouse *CNKSR2* in the lateral forebrain was not sufficient to decrease cell proliferation in the ectopic location. Possible explanations for this observation are: (1) the context in the lateral forebrain is different from that of the roof plate with respect to the regulation of cell proliferation; (2) different levels of *CNKSR2* might be required to effect the desired changes (Peyssonnaux and Eychène, 2001); and/or (3) there are other downstream effector(s) of RA signaling that work in combination with *CNKSR2* to regulate cell proliferation in the forebrain roof plate (Ito et al., 2021).

It is possible that patterning of the forebrain roof plate results in the differential cell proliferation observed across this region. Thus, the likely cause of the increase in cell proliferation and pMEK1/2-positive cells upon knockdown of *CNKSR2* could be a result of altered patterning of the invaginating forebrain roof plate. This was supported by the observed changes in expression of the markers *Bmp7*, *Wnt7b*, *Zic2* and *Otx2* upon knockdown of *CNKSR2*. We hypothesized that *CNKSR2* modulates the levels of the Ras/Raf/MEK signaling and thereby patterns the roof plate (expression of markers), which in turn drives its invagination. In support of this, we observed that co-electroporation of *CNKSR2*-RNAi with dominant-negative MKK1 not only rescues the invagination defect and the normal expression pattern of the midline marker *Bmp7*, but also

Development (2023) 150, dev200857. doi:10.1242/dev.200857

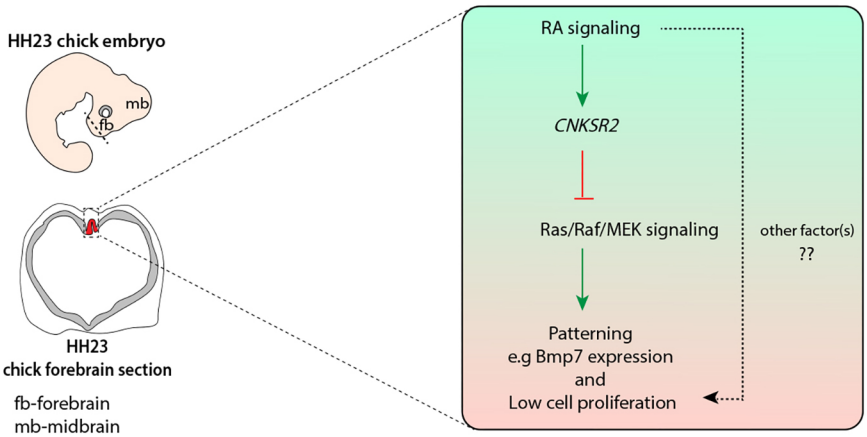

Fig. 7. Model illustrating the mechanism of action of *CNKSR2* in the invaginating forebrain roof plate. Schematic of the mode of action of *CNKSR2* in the chick forebrain roof plate. RA signaling regulates the expression of *CNKSR2*, downregulating the Ras/Raf/MEK signaling in the invaginating roof plate midline. These low levels of Ras/Raf/MEK signaling are essential for the expression of roof plate markers, such as *Bmp7*, for low cell proliferation in the midline and for subsequent invagination of the roof plate. Moreover, RA signaling, possibly in conjunction with other factor(s), may regulate cell proliferation in the invaginating roof plate midline through a yet to be identified mechanism.

restores the domain of reduced Ras/Raf/ MEK signaling and reduced cell proliferation in the midline. Interestingly, the inhibition of Ras/Raf/MEK signaling in the lateral forebrain was sufficient for the expression of the midline marker *Bmp7* but not sufficient for reducing cell proliferation. This suggests that differences exist between the context of the roof plate and the lateral forebrain, and that other factors, besides Ras/Raf/MEK signaling (which functions downstream of RA and/or *CNKSR2*) are likely to be important for the reduction in cell proliferation observed in the roof plate midline.

In the zebrafish model for HPE, it has been demonstrated that *tgif1*, one of the genes linked to HPE, is involved in regulating RA signaling during early patterning of the forebrain. Additionally, the loss of function of Cyp26a1, a retinoic acid-degrading enzyme, in the forebrain phenocopies the *tgif1* morphants (Gongal and Waskiewicz, 2008). In addition, various studies in quails (Maden et al., 1996), swine (Hale, 1933), mice (Halilagic et al., 2007; Ribes et al., 2006), chick and zebrafish (Begemann et al., 2001; Maves and Kimmel, 2005) show that either lowering or increasing the levels of RA signaling can lead to forebrain defects, which includes HPE-like phenotypes (Gongal et al., 2011).

The forebrains of the RA signaling reporter (RARE-LacZ) mice do not show the presence of any RA signaling in the forebrain roof plate midline (Rossant et al., 1991). Moreover, mice lacking sources of RA (Mic et al., 2004; Molotkova et al., 2007) show normal roof plate invagination, unlike our observations of the chick forebrain (Gupta and Sen, 2015). In addition, there are no reports of *CNKSR2* expression in the forebrain roof plate midline in mice. Taken together, this indicates that the RA signaling-*CNKSR2* axis might not be involved in regulation of forebrain roof plate invagination in mice. However, it is possible that mice may have diverged during evolution, and the role of RA signaling and *CNKSR2* in regulating forebrain roof plate may be conserved in humans. To date, there is no study suggesting a link between the loss of function of *CNKSR2* and HPE in humans, although the loss of *CNKSR2* is attributed to phenotypes such as microcephaly, cortical atrophy and intellectual disability (Polla et al., 2019). There is a possibility that *CNKSR2* could be acting through a non-cell-autonomous manner on the process of midline invagination, probably through the action of other signaling pathways present in this region, such as Bmp signaling and Wnt signaling (Furuta et al., 1997; Lee et al., 2000). However, an in-depth analysis into this aspect is required to confirm this possibility. In total, there is a need for further investigation to establish a link between RA signaling and/or *CNKSR2*, and HPE.

In conclusion, our results reveal that the phenotypes caused by the loss of function of *CNKSR2* in the chick forebrain roof plate are like those observed with the loss of RA signaling. We postulate that RA and/or *CNKSR2* regulates roof plate patterning through modulation of Ras/Raf/MEK signaling, which in turn drives the process of roof plate invagination (Fig. 7). Moreover, our study is the first to identify *CNKSR2* as a downstream mediator of RA signaling, opening the possibility that this mechanism of regulating morphogenesis may exist in other contexts besides the chick forebrain roof plate.

MATERIALS AND METHODS

Chicken eggs and embryos

Fertilized White leghorn (*Gallus gallus*) eggs were obtained from the following sources: (1) Central Avian Research Institute (CARI), Bareilly, Uttar Pradesh, India; and (2) Ganesh Enterprises, Nankari Village, Kanpur, Uttar Pradesh, India. The eggs were incubated at 38°C in a humidified incubator until the desired stages. The embryos were staged according to Hamburger and Hamilton (Hamburger and Hamilton, 1951).

Tissue preparation

Heads from unmanipulated and electroporated chicken embryos were harvested at the desired stage and fixed in 4% PFA (paraformaldehyde) overnight. The heads were cryoprotected by passing through a gradient of 15% sucrose and 30% sucrose prepared in PBS (phosphate-buffered saline). The heads were then embedded in Polyfreeze/OCT (Sigma, SHH0026) and 10 µm coronal sections were generated using a cryostat (Leica CM1850).

Plasmids used in this study

pCIG-VP16RARα-IRES-nGFP was a gift from Thomas Jessell (Addgene plasmid #16287) (Novitch et al., 2003). pCAGEN-RAR403 and pCAG-GFP were gifts from Prof. Constance Cepko (Harvard Medical School, Boston, MA, USA). cDNA clones for *Bmp7* and *Wnt7b* were gifts from Prof. Clifford Tabin (Harvard Medical School, Boston, MA, USA). pRARE-AP, cDNA for *Otx2* and *Zic2* (RT-PCR amplified) constructs have been described previously (Gupta and Sen, 2015). The cDNA for *CNKSR2* (ChEST 713i22) was obtained from the chicken EST collection from Source Bioscience (previously MRC Geneservice, UK). The top and bottom strands of the RNAi-containing region of *CNKSR2* (*CNKSR2*-RNAi) were synthesized (Macrogen), annealed and cloned into the pRmiR vector after BsaI digestion (Smith et al., 2009): top strand sequence, 5′-TGCTG**TGTACAGGCAACAGACTAAAG**GTTTTGGCCACTGAC-TGACCTTTAGTCTTGCCTGTACA-3′; bottom strand sequence, 5′-CCT-GTGTACAGGCAAGACTAAAGGTCAGTCAGTGGCCAAAAC**CTTT-AGTCTGTTGCCTGTACA**C-3′ (bold indicates the region in *CNKSR2* mRNA that is targeted by the designed RNAi construct).

Sensor-*CNKSR2* was generated by first excising the putative target region from EST using the enzymes NotI and HindIII, and then ligating it with the pCAG-mCherry vector (a gift from Prof. Constance Cepko) between NotI and HindIII restriction sites. pCAG-m*CNKSR2* was generated by

Development (2023) 150, dev200857. doi:10.1242/dev.200857

amplifying the MGC clone (ThermoFisher Scientific, USA) for *CNKSR2* (IRAV-158g9) with the primers (forward) 5′-CTAGTCTAGAATGGCTCTGATAATGGAAC-3′ with XbaI site and (reverse) 5′-CGAATGCGGCCGCTTACACATGTGTCTCAATG-3′ with the NotI site, and cloned into the pCAG-MCS backbone digested with XbaI and NotI. TA-m*CNKSR2*-CDS was generated by PCR amplifying the MGC clone (ThermoFisher Scientific) for *CNKSR2* (IRAV-158g9) with the primers (forward) 5′-GGGTTCAACCATTGCTGTCT-3′ and (reverse) 5′-TTACACATGTGTCTCAATGTATG-3′, and cloned into the TA vector [ThermoFisher Scientific, K207020 (previously 45-0007LT)] according to the manufacturer's protocol.

pCIG-MKK1dn was a gift from Prof. Olivier Pourquié (Harvard Medical School, Boston, MA, USA). pcDNA3-HRasV12 was a gift from Julian Downward (Addgene plasmid #39504) (Rodriguez-Viciana et al., 1997).

Cell culture

Human embryonic kidney (HEK-293T, ATCC CRL-3216) fibroblast cell lines were cultured in Dulbecco's Modified Eagle's Medium (DMEM) (Sigma, D7777) with 10% fetal bovine serum.

Sensor assay

Human embryonic kidney fibroblast 293T cells at 60-70% confluency was transfected using Turbofect (ThermoFisher Scientific, R0531) according to the manufacturer's protocol, with pRmiR vector(s) and Sensor-*CNKSR2* in a 6:1 molar ratio. GFP and mCherry fluorescence were observed after 72 h.

In ovo electroporation

After incubating the eggs for 24 h, 2-3 ml of albumin was taken out to lower the developing chick embryo. A window was then created on the top of the egg and DNA constructs (1 µg/µl-2 µg/µl) with 0.1% of Fast Green (Sigma-Aldrich, 44715) were injected into the forebrain vesicle at HH10 and HH18. Platinum hockey stick electrodes (NepaGene, CUY611P3-1) were positioned on this forebrain vesicle such that the positive electrode was placed over the dorsal forebrain, while the negative electrode was placed below the yolk of the egg at HH10 and HH18, and the electrodes were placed close to each other. Five electric pulses of 15 V each for embryos at HH10 and HH18 were applied for the 50 ms duration with a gap of 950 ms, using a square wave pulse electroporator (Nepa Gene, CUY21SC). Sterile PBS containing penicillin and streptomycin was layered over the embryos and the egg was sealed with tape. Eggs were put back into the egg incubator until the desired HH stage of development and then harvested for tissue section preparation.

Alkaline phosphatase staining

The slides were fixed for 5 min in 4% PFA, followed by the quenching of endogenous alkaline phosphatase (AP) by incubating the slides in PBS at 65°C for 1 h. The slides were then equilibrated in the NTM buffer [100 mM Tris (pH 9.5), 100 mM NaCl, 50 mM $MgCl_2$ and 0.1% Tween 20] for 10 min and then incubated in the NTM buffer containing the substrates BCIP and NBT. The reaction was monitored intermittently for the development of colored precipitate and stopped by adding 4% PFA. Image acquisition was performed using a Leica DM500B microscope equipped with a DFC500 camera.

RNA *in situ* hybridization

RNA hybridization was performed on coronal sections of embryonic chick forebrain according to established protocols (Trimarchi et al., 2007). The digoxigenin-labeled riboprobes for RNA *in situ* hybridization were generated from the cDNA clones mentioned in the previous section by *in vitro* transcription.

Immunofluorescence staining

We used an established protocol for immunostaining. Briefly, after a 5 min fixation in 4% PFA, three washes with PBS were carried out followed by 1 h of blocking with 5% of heat-inactivated goat serum (HINGS) in PBS. After that, the primary antibody at the required dilution was layered on the slide in the blocking reagent and incubated overnight at 4°C. The primary antibodies were used at the following concentrations: anti-pMEK1/2 antibody, 1:200 (CST, 9121), anti-PH3 antibody, 1:1000 (Sigma-Aldrich, H0412) and anti-GFP 1:300 (ThermoFisher Scientific, A-6455). Slides were then washed three times in PBS for 5 min each and the secondary antibody (1:250) was layered on the slides followed by incubation for 2 h at room temperature. The secondary antibodies used were as follows: Alexa Fluor 488-conjugated anti-rabbit IgG (Jackson ImmunoResearch Laboratories, 111-545-003) and Alexa Fluor 594-conjugated anti-rabbit IgG (Jackson ImmunoResearch Laboratories, 111-585-045).

EdU labeling and detection

For EdU detection, fertilized chicken eggs were electroporated with either pRmiR-empty (control) or *CNKSR2*-RNAi (treatment) in the forebrain vesicle at HH10, incubated for the desired time and then overlaid with 25 µg in 200 µl PBS (0.5 mM of EdU) of the thymidine analog EdU (ThermoFisher Scientific, C10338) and harvested at HH23. Brains were harvested from embryos 2 h after EdU overlay, fixed in 4% PFA, dehydrated in 15% and 30% sucrose in PBS, and embedded in OCT. 10 µm frozen sections from these brains were processed for EdU detection using the CLICK-IT EdU-labeling kit (ThermoFisher Scientific, C10338) according to the manufacturer's protocol.

TUNEL assay

TUNEL assay was performed on either pRmiR-empty or *CNKSR2*-RNAi electroporated forebrains at HH18 or HH23, according to the manufacturer's protocol (Roche, 12156792910).

Image acquisition

A Leica stereomicroscope (DM500B) equipped with a DFC500 camera was used to capture RNA *in situ* hybridization images and fluorescent images.

Quantification and statistical analysis

Percentage of different phenotypes upon knockdown of *CNKSR2* in the roof plate in Fig. 3

All control electroporated embryos were considered normal as the roof plate invaginated in a W-shape. DAPI stained *CNKSR2*-RNAi electroporated forebrain sections were analyzed for either a flat or a U/V-shaped roof plate phenotype, solely based on morphology (n=29 embryos) using Photoshop CS6. Out of these 29 embryos, 16 embryos showed U/V-shaped invagination (55.17%), while the remaining 13 embryos (44.83%) showed a flat roof plate phenotype. Both the values were then plotted as a pie chart using GraphPad 8.0.2 (v.263) software.

PH3-, EdU- and pMEK1/2-positive cells in Figs 4 and 6

A rectangle of 60×75 µm^2 was drawn in the 20× magnification of the image, and the number of double-positive cells (red, immunostaining; green, GFP) was counted manually in Photoshop CS6. The number of DAPI cells was counted using ImageJ software and the percentage was calculated in three sections each of five embryos and averaged (n=5 each for test and control). As we were assessing the differences between two groups, control and test, we performed statistical analyses using an unpaired t-test and then plotted the graphs using GraphPad 8.0.2 (v.263) software in Figs 4D,H and 6C. For Fig. 6K, statistical analyses were performed using one-way ANOVA with Sidak's multiple comparison test using GraphPad 8.0.2 (v.263) software to compare means between pCAG-GFP versus *CNKSR2*-RNAi, MKK1-dn-IRES-GFP versus *CNKSR2*-RNAi+MKK1-dn, m*CNKSR2* versus *CNKSR2*-RNAi+m*CNKSR2*,*CNKSR2*-RNAi versus *CNKSR2*-RNAi+MKK1-dn, and *CNKSR2*-RNAi versus *CNKSR2*-RNAi+m*CNKSR2*. The values are represented as bar graphs, plotted using GraphPad 8.0.2 (v.263) software.

TUNEL- and PH3-positive cells in Figs S3 and S4

A rectangle of 13×44 µm^2 was drawn in the 20× magnification of the image and the number of double-positive (red, immunostaining; green, GFP) cells was counted manually in Photoshop CS6. The number of DAPI cells was counted using ImageJ software and the percentages of TUNEL- and PH3-positive cells were calculated in two or three sections each of three embryos and averaged. As we were assessing the differences between two groups,

control and test, we performed statistical analyses using an unpaired *t*-test and then plotted the graphs using GraphPad 8.0.2 (v.263) software.

Quantification of expression domains of Zic2 and Otx2 in Fig. 5

The expression domains of *Zic2* and *Otx2* were quantified by ImageJ on sections of four embryos electroporated with either control or *CNKSR2*-RNAi. The values were averaged and plotted as bar graphs using GraphPad 8.0.2 (v.263) software. Statistical analysis was performed using an unpaired *t*-test and significance was obtained.

Acknowledgements

The authors acknowledge Prof. C. Cepko (Harvard Medical School, Boston, MA, USA) for constructs related to RA signaling. The authors also acknowledge Prof. Olivier Pourquié (Harvard Medical School, Boston, MA, USA) for the pCIG-MKK1dn construct. The authors acknowledge the technical assistance of Ms Shruti Jain, Mr Kaustuv Ghosh and Ms Archita Mishra with this study. The authors thank Prof. Amitabha Bandyopadhyay, Dr Sandeep Gupta, Dr Suvimal Kumar Sindhu and Dr Tathagata Biswas for their critical comments on this manuscript. The authors thank Mr Naresh Gupta for his technical support with this study.

Competing interests

The authors declare no competing or financial interests.

Author contributions

Conceptualization: N.U., M.A.A.Z., J.S.; Methodology: N.U., M.A.A.Z., J.S.; Validation: N.U., M.A.A.Z., A.R., J.S.; Formal analysis: N.U., M.A.A.Z., A.R., J.S.; Investigation: N.U., J.S.; Resources: N.U., J.S.; Data curation: N.U., J.S.; Writing - original draft: N.U., J.S.; Writing - review & editing: N.U., A.R., J.S.; Visualization: N.U., J.S.; Supervision: J.S.; Project administration: J.S.; Funding acquisition: J.S.

Funding

This work was supported by a grant from the Department of Biotechnology, Government of India (BT/PR23629/MED/97/376/2017 to J.S.). N.U., M.A.A.Z. and A.R. are supported by the Ministry of Human Resources and Development, Government of India.

Data availability

All relevant data can be found within the article and its supplementary information.

Peer review history

The peer review history is available online at https://journals.biologists.com/dev/lookup/doi/10.1242/dev.200857.reviewer-comments.pdf

References

Begemann, G., Schilling, T. F., Rauch, G.-J., Geisler, R. and Ingham, P. W. (2001). The zebrafish *neckless* mutation reveals a requirement for *raldh2* in mesodermal signals that pattern the hindbrain. *Development* **128**, 3081-3094. doi:10.1242/dev.128.16.3081

Crowe, D. L., Kim, R. and Chandraratna, R. A. S. (2003). Retinoic acid differentially regulates cancer cell proliferation via dose-dependent modulation of the mitogen-activated protein kinase pathway. *Mol. Cancer Res.* **1**, 532-540.

Damiano, J. A., Burgess, R., Kivity, S., Lerman-Sagie, T., Afawi, Z., Scheffer, I. E., Berkovic, S. F. and Hildebrand, M. S. (2017). Frequency of *CNKSR2* mutation in the X-linked epilepsy-aphasia spectrum. *Epilepsia* **58**, e40-e43. doi:10.1111/epi.13666

Daoqi, M., Guohong, C., Yuan, W., Zhixiao, Y., Kaili, X. and Shiyue, M. (2020). Exons deletion of CNKSR2 gene identified in X-linked syndromic intellectual disability. *BMC Med. Genet.* **21**, 69. doi:10.1186/s12881-020-01004-2

Delfini, M.-C., Dubrulle, J., Malapert, P., Chal, J. and Pourquié, O. (2005). Control of the segmentation process by graded MAPK/ERK activation in the chick embryo. *Proc. Natl. Acad. Sci. USA* **102**, 11343-11348. doi:10.1073/pnas.0502933102

Dubourg, C., Bendavid, C., Pasquier, L., Henry, C., Odent, S. and David, V. (2007). Holoprosencephaly. *Orphanet J. Rare Dis.* **2**, 8. doi:10.1186/1750-1172-2-8

Dupe, V., Rochard, L., Mercier, S., Le Petillon, Y., Gicquel, I., Bendavid, C., Bourrouillou, G., Kini, U., Thauvin-Robinet, C., Bohan, T. P. et al. (2011). NOTCH, a new signaling pathway implicated in holoprosencephaly. *Hum. Mol. Genet.* **20**, 1122-1131. doi:10.1093/hmg/ddq556

Erata, E., Gao, Y., Purkey, A. M., Soderblom, E. J., Mcnamara, J. O. and Soderling, S. H. (2021). Cnksr2 loss in mice leads to increased neural activity and behavioral phenotypes of epilepsy-aphasia syndrome. *J. Neurosci.* **41**, 9633-9649. doi:10.1523/JNEUROSCI.0650-21.2021

Furuta, Y., Piston, D. W. and Hogan, B. L. M. (1997). Bone morphogenetic proteins (BMPs) as regulators of dorsal forebrain development. *Development* **124**, 2203-2212. doi:10.1242/dev.124.11.2203

Geng, X. and Oliver, G. (2009). Pathogenesis of holoprosencephaly. *J. Clin. Investig.* **119**, 1403-1413. doi:10.1172/JCI38937

Gongal, P. A. and Waskiewicz, A. J. (2008). Zebrafish model of holoprosencephaly demonstrates a key role for TGIF in regulating retinoic acid metabolism. *Hum. Mol. Genet.* **17**, 525-538. doi:10.1093/hmg/ddm328

Gongal, P. A., French, C. R. and Waskiewicz, A. J. (2011). Aberrant forebrain signaling during early development underlies the generation of holoprosencephaly and coloboma. *Biochim. Biophys. (BBA) – Mol. Basis Dis.* **1812**, 390-401. doi:10.1016/j.bbadis.2010.09.005

Gupta, S. and Sen, J. (2015). Retinoic acid signaling regulates development of the dorsal forebrain midline and the choroid plexus in the chick. *Development* **142**, 1293-1298. doi:10.1242/dev.122390

Hale, F. (1933). Pigs born without eye balls. In *Problems of birth defects* (ed. T. V. N. Persaud), pp. 166-167. Dordrecht: Springer.

Halilagic, A., Ribes, V., Ghyselinck, N. B., Zile, M. H., Dollé, P. and Studer, M. (2007). Retinoids control anterior and dorsal properties in the developing forebrain. *Dev. Biol.* **303**, 362-375. doi:10.1016/j.ydbio.2006.11.021

Hamburger, V. and Hamilton, H. L. (1951). A series of normal stages in the development of the chick embryo. *J. Morphol.* **88**, 49-92. doi:10.1002/jmor.1050880104

Higa, L. A., Wardley, J., Wardley, C., Singh, S., Foster, T. and Shen, J. J. (2021). CNKSR2-related neurodevelopmental and epilepsy disorder: a cohort of 13 new families and literature review indicating a predominance of loss of function pathogenic variants. *BMC Med. Genomics* **14**, 186. doi:10.1186/s12920-021-01033-7

Houge, G., Rasmussen, I. H. and Hovland, R. (2011). Loss-of-function CNKSR2 mutation is a likely cause of non-syndromic X-linked intellectual disability. *Mol. Syndromol.* **2**, 60-63. doi:10.1159/000335159

Ishiguro, A., Hatayama, M., Otsuka, M. I. and Aruga, J. (2018). Link between the causative genes of holoprosencephaly: Zic2 directly regulates Tgif1 expression. *Sci. Rep.* **8**, 2140. doi:10.1038/s41598-018-20242-2

Ito, H., Morishita, R., Noda, M., Ishiguro, T., Nishikawa, M. and Nagata, K.-I. (2021). The synaptic scaffolding protein CNKSR2 interacts with CYTH2 to mediate hippocampal granule cell development. *J. Biol. Chem.* **297**, 101427. doi:10.1016/j.jbc.2021.101427

Keaton, A. A., Solomon, B. D., Kauvar, E. F., El-Jaick, K. B., Gropman, A. L., Zafer, Y., Meck, J. M., Bale, S. J., Grange, D. K., Haddad, B. R. et al. (2010). TGIF mutations in human holoprosencephaly: correlation between genotype and phenotype. *Mol. Syndromol.* **1**, 211-222. doi:10.1159/000328203

Krauss, R. S. (2007). Holoprosencephaly: new models, new insights. *Expert Rev. Mol. Med.* **9**, 1-17. doi:10.1017/S1462399407000440

Lee, S. M., Tole, S., Grove, E. and Mcmahon, A. P. (2000). A local Wnt-3a signal is required for development of the mammalian hippocampus. *Development* **127**, 457-467. doi:10.1242/dev.127.3.457

Maden, M., Gale, E., Kostetskii, I. and Zile, M. (1996). Vitamin A-deficient quail embryos have half a hindbrain and other neural defects. *Curr. Biol.* **6**, 417-426. doi:10.1016/S0960-9822(02)00509-2

Maves, L. and Kimmel, C. B. (2005). Dynamic and sequential patterning of the zebrafish posterior hindbrain by retinoic acid. *Dev. Biol.* **285**, 593-605. doi:10.1016/j.ydbio.2005.07.015

Mic, F. A., Molotkov, A., Molotkova, N. and Duester, G. (2004). Raldh2 expression in optic vesicle generates a retinoic acid signal needed for invagination of retina during optic cup formation. *Dev. Dyn.* **231**, 270-277. doi:10.1002/dvdy.20128

Molotkova, N., Molotkov, A. and Duester, G. (2007). Role of retinoic acid during forebrain development begins late when Raldh3 generates retinoic acid in the ventral subventricular zone. *Dev. Biol.* **303**, 601-610. doi:10.1016/j.ydbio.2006.11.035

Nakagawa, S., Fujii, T., Yokoyama, G., Kazanietz, M. G., Yamana, H. and Shirouzu, K. (2003). Cell growth inhibition by all-trans retinoic acid in SKBR-3 breast cancer cells: involvement of protein kinase C? And extracellular signal-regulated kinase mitogen-activated protein kinase. *Mol. Carcinog.* **38**, 106-116. doi:10.1002/mc.10150

Nanni, L., Ming, J. E., Bocian, M., Steinhaus, K., Bianchi, D. W., De Die-Smulders, C., Giannotti, A., Imaizumi, K., Jones, K. L., Del Campo, M. et al. (1999). The mutational spectrum of the Sonic Hedgehog gene in holoprosencephaly: SHH mutations cause a significant proportion of autosomal dominant holoprosencephaly. *Hum. Mol. Genet.* **8**, 2479-2488. doi:10.1093/hmg/8.13.2479

Novitch, B. G., Wichterle, H., Jessell, T. M. and Sockanathan, S. (2003). A requirement for retinoic acid-mediated transcriptional activation in ventral neural patterning and motor neuron specification. *Neuron* **40**, 81-95. doi:10.1016/j.neuron.2003.08.006

Petryk, A., Graf, D. and Marcucio, R. (2015). Holoprosencephaly: signaling interactions between the brain and the face, the environment and the genes, and the phenotypic variability in animal models and humans. *Wiley Interdiscip. Rev. Dev. Biol.* **4**, 17-32. doi:10.1002/wdev.161

Peyssonnaux, C. and Eychène, A. (2001). The Raf/MEK/ERK pathway: new concepts of activation. *Biol. Cell* **93**, 53-62. doi:10.1016/S0248-4900(01)01125-X

Polla, D. L., Saunders, H. R., Vries, B. B. A., Bokhoven, H. and Brouwer, A. P. M. (2019). A de novo variant in the X–linked gene *CNKSR2* is associated with seizures and mild intellectual disability in a female patient. *Mol. Genet. Genomic Med.* **7**, e00861. doi:10.1002/mgg3.861

Ribeiro, L. A., El-Jaick, K. B., Muenke, M. and Richieri-Costa, A. (2006). SIX3 mutations with holoprosencephaly. *Am. J. Med. Genet. A* **140A**, 2577-2583. doi:10.1002/ajmg.a.31377

Ribes, V., Wang, Z., Dollé, P. and Niederreither, K. (2006). Retinaldehyde dehydrogenase 2 (RALDH2)-mediated retinoic acid synthesis regulates early mouse embryonic forebrain development by controlling FGF and sonic hedgehog signaling. *Development* **133**, 351-361. doi:10.1242/dev.02204

Rodriguez-Viciana, P., Warne, P. H., Khwaja, A., Marte, B. M., Pappin, D., Das, P., Waterfield, M. D., Ridley, A. and Downward, J. (1997). Role of phosphoinositide 3-OH kinase in cell transformation and control of the actin cytoskeleton by ras. *Cell* **89**, 457-467. doi:10.1016/S0092-8674(00)80226-3

Roessler, E. and Muenke, M. (2010). The molecular genetics of holoprosencephaly. *Am. J. Med. Genet. C Semin. Med. Genet.* **154C**, 52-61. doi:10.1002/ajmg.c.30236

Rossant, J., Zirngibl, R., Cado, D., Shago, M. and Giguère, V. (1991). Expression of a retinoic acid response element-hsplacZ transgene defines specific domains of transcriptional activity during mouse embryogenesis. *Genes Dev.* **5**, 1333-1344. doi:10.1101/gad.5.8.1333

Roy, P., Kumar, B., Shende, A., Singh, A., Meena, A., Ghosal, R., Ranganathan, M. and Bandyopadhyay, A. (2013). A genome-wide screen indicates correlation between differentiation and expression of metabolism related genes. *PLoS One* **8**, e63670. doi:10.1371/journal.pone.0063670

Sindhu, S. K., Udaykumar, N., Zaidi, M. A. A., Soni, A. and Sen, J. (2019). MicroRNA-19b restricts Wnt7b to the hem, which induces aspects of hippocampus development in the avian forebrain. *Development* **146**, dev175729. doi:10.1242/dev.175729

Smith, C. A., Roeszler, K. N., Ohnesorg, T., Cummins, D. M., Farlie, P. G., Doran, T. J. and Sinclair, A. H. (2009). The avian Z-linked gene DMRT1 is required for male sex determination in the chicken. *Nature* **461**, 267-271. doi:10.1038/nature08298

Sun, Y., Liu, Y.-D., Xu, Z.-F., Kong, Q.-X. and Wang, Y.-L. (2018). *CNKSR2* mutation causes the X-linked epilepsy-aphasia syndrome: a case report and review of literature. *World J. Clin. Cases* **6**, 570-576. doi:10.12998/wjcc.v6.i12.570

Sundaram, M. and Han, M. (1995). The C. elegans ksr-1 gene encodes a novel raf-related kinase involved in Ras-mediated signal transduction. *Cell* **83**, 889-901. doi:10.1016/0092-8674(95)90205-8

Therrien, M., Wong, A. M. and Rubin, G. M. (1998). CNK, a RAF-binding multidomain protein required for RAS signaling. *Cell* **95**, 343-353. doi:10.1016/S0092-8674(00)81766-3

Trimarchi, J. M., Stadler, M. B., Roska, B., Billings, N., Sun, B., Bartch, B. and Cepko, C. L. (2007). Molecular heterogeneity of developing retinal ganglion and amacrine cells revealed through single cell gene expression profiling. *J. Comp. Neurol.* **502**, 1047-1065. doi:10.1002/cne.21368

Vaags, A. K., Bowdin, S., Smith, M.-L., Gilbert-Dussardier, B., Brocke-Holmefjord, K. S., Sinopoli, K., Gilles, C., Haaland, T. B., Vincent-Delorme, C., Lagrue, E. et al. (2014). Absent CNKSR2 causes seizures and intellectual, attention, and language deficits. *Ann. Neurol.* **76**, 758-764. doi:10.1002/ana.24274

Wang, J. and Yen, A. (2008). A MAPK-positive feedback mechanism for BLR1 signaling propels retinoic acid-triggered differentiation and cell cycle arrest. *J. Biol. Chem.* **283**, 4375-4386. doi:10.1074/jbc.M708471200

Weiss, K., Kruszka, P., Guillen Sacoto, M. J., Addissie, Y. A., Hadley, D. W., Hadsall, C. K., Stokes, B., Hu, P., Roessler, E., Solomon, B. et al. (2018). In-depth investigations of adolescents and adults with holoprosencephaly identify unique characteristics. *Genet. Med.* **20**, 14-23. doi:10.1038/gim.2017.68